Computers and Concrete, *Vol. 13, No. 2 (2014) 187-207*
DOI: http://dx.doi.org/10.12989/cac.2014.13.2.187

Chloride diffusivity of concrete: probabilistic characteristics at meso-scale

Zichao Pan[1,2a], Xin Ruan[*1] and Airong Chen[1b]

[1]*Department of Bridge Engineering*, *Tongji University*, *Shanghai*, *200092*, *China*
[2]*Department of Civil and Environmental Engineering*, *University of California at Berkeley*, *CA*, *94720*, *USA*

(*Received June 5, 2013, Revised October 1, 2013, Accepted October 6, 2013*)

Abstract. This paper mainly discusses the influence of the aggregate properties including grading, shape, content and distribution on the chloride diffusion coefficient, as well as the initiation time of steel corrosion from a probabilistic point of view. Towards this goal, a simulation method of random aggregate structure (RAS) based on elliptical particles and a procedure of finite element analysis (FEA) at meso-scale are firstly developed to perform the analysis. Next, the chloride diffusion coefficient ratio between concrete and cement paste D_{app}/D_{cp} is chosen as the index to represent the effect of aggregates on the chloride diffusion process. Identification of the random distribution of this index demonstrates that it can be viewed as actually having a normal distribution. After that, the effect of aggregates on D_{app}/D_{cp} is comprehensively studied, showing that the appropriate properties of aggregates should be decided by both of the average and the deviation of D_{app}/D_{cp}. Finally, a case study is conducted to demonstrate the application of this mesoscopic method in predicting the initiation time of steel corrosion in reinforced concrete (RC) structures. The mesoscopic probabilistic method developed in this paper can not only provide more reliable evidences on the proper grading and shape of aggregates, but also play an important role in the probability-based design method.

Keywords: concrete structures; durability; mathematical modeling; uncertainty

1. Introduction

Steel corrosion is one of the most significant problems to reinforced concrete (RC) members. When the steel rebar embedded in the concrete starts to corrode, the concrete surrounding the rebar will be cracked due to the expansion of the corrosion products. As a result, the bonding property of the steel rebar, as well as its cooperative working performance with concrete, can be greatly affected (Cabrera 1996, Almusallam *et al*. 1996). Furthermore, some experimental research reported that the steel corrosion process could decrease the tensile strength of the steel rebar itself (Du *et al*. 2005, Cairns *et al*. 2005). Therefore, the steel corrosion process can rapidly decrease the loading capacity of RC members, which will result in a series of safety problems.

∗Corresponding author, Associate Professor, E-mail: ruanxin@tongji.edu.cn
[a]Ph.D Student, E-mail: panzichao@gmail.com
[b]Professor, E-mail: a.chen@tongji.edu.cn

http://www.techno-press.org/?journal=cac&subpage=8 ISSN: 1598-8198 (Print), 1598-818X (Online)

In chlorine environment like coastal region or where deicing salt is used, the steel corrosion is mainly induced by the diffusion process of chloride ions. As the chloride ions accumulate at the surface of the steel rebar, the passivation layer which can prevent the rebar from corroding will become unstable. When the chloride concentration near the rebar reaches a threshold value, the passivation layer starts to dissolve, resulting in the initiation of steel corrosion. Based on the Fick's diffusion law, the initiation time of steel corrosion can be calculated by the following equation.

$$T_{\text{corr}} = \frac{x_s^2}{\pi \cdot D_{\text{app}}} \cdot \frac{(C_s - C_0)^2}{(C_s - C_c)^2} \tag{1}$$

where x_s is the position of the steel rebar. C_s, C_0 and C_c are the surface, initial and threshold chloride concentrations, respectively. D_{app} is the apparent chloride diffusion coefficient.

To obtain the corrosion initiation time by Eq. (1), numerous efforts were made to determine the apparent diffusion coefficient D_{app} (Garboczi and Bentz 1992, Halamickova *et al*. 1995, Xi and Bazant 1999, Ababneh *et al*. 2003, Oh and Jang 2004, Saetta 2005, Bentz 2007, Han 2007, Van Mien *et al*. 2011, Wang and Ueda 2011, Li *et al*. 2012, Zhangand Zhao 2012, Wang *et al*. 2012, Zhang *et al*. 2013). Generally, this parameter can be influenced by a lot of factors, such as concrete porosity, temperature, relative humidity, aggregate content, etc. Currently, these parameters are often taken into account by a so-called multifactor method (Xi and Bazant 1999, Shafei *et al*. 2011). The general idea of this method is to set up a reference diffusion coefficient in a standard condition and then describe the above influences by multiplying the reference diffusion coefficient with independent functions. The general model of the multifactor method can be described by the following equation.

$$D_{\text{app}} = D_0(x_1^0, x_2^0, \dots, x_n^0) \cdot f_1(x_1) \cdot f_2(x_2) \cdots f_n(x_n) \tag{2}$$

where $x_1 \sim x_n$ are factors that affect the apparent diffusion coefficient. These factors can be classified into two types: environmental factors (e.g., temperature, relative humidity, etc.) and factors innate to the material itself (e.g., cement type, mix proportion of concrete, etc.). $x_1^0 \sim x_n^0$ are the values of $x_1 \sim x_n$, with which the reference diffusion coefficient D_0 is measured, and $f_1 \sim f_n$ are independent functions derived quantitatively describing how the factors of $x_1 \sim x_n$ influence the apparent chloride diffusion coefficient.

Up to now, most of the above factors have been widely discussed and the expressions of their independent functions were given in many papers (Xi and Bazant 1999, Ababneh *et al*. 2003, Saetta 2005, Chen and Mahadevan 2008). However, the influence of the aggregates on D_{app} is still not sufficiently discussed. Although some quantitative models have been already proposed either by experimental method (Yang and Su 2002, Caré 2003, Yang 2005) or theoretical method (Hobbs 1999, Caré and Hervé 2004, Zheng and Zhou 2008, Li *et al*. 2012), most of these models only adopted the aggregate content as the only parameter, while the influences of the aggregate shape, grading, etc. were ignored. Furthermore, the current approach to consider the influence of aggregates on the chloride diffusion process as well as the corrosion initiation time was mainly conducted in a deterministic way, where the probabilistic property caused by the random distribution of aggregates in cement paste was not considered. The above deficiencies are mainly caused by the current macro-scale analysis method, where concrete is considered as a homogenous material. Therefore, to discuss the influences of the aggregate shape, grading and especially the random distribution on the diffusion process of chloride ions, as well as the corrosion initiation

time of steel rebars, the analysis should be conducted at mesoscale, where concrete is considered as a composite material in which the aggregates can be explicitly simulated (Zeng 2007, Ruan and Pan 2012).

This paper mainly discusses the influence of the aggregate grading, shape, content and distribution on the chloride diffusivity, as well as the corrosion initiation time in a probabilistic way. Towards this goal, simulation method of random elliptical aggregates and the procedure of mesoscopic finite element analysis are introduced in the first and second parts of this paper, respectively. The chloride diffusion coefficient ratio in concrete and in cement paste $D_{\text{app}}/D_{\text{cp}}$ is chosen as the index to represent the effect of aggregate on the chloride diffusion process at macro-scale. In the third part of this research, the random distribution of $D_{\text{app}}/D_{\text{cp}}$ is identified. The effects of aggregates, including aggregate grading, aggregate shape, size of meso-scale model, aggregate content, on $D_{\text{app}}/D_{\text{cp}}$, are studied. Finally, a case study is conducted to demonstrate the application of this mesoscopic method in predicting the initiation time of steel corrosion.

2. Meso-scale model

2.1 Generation of elliptical particles

At meso-scale, concrete is usually considered as a composite material, where the aggregates are randomly distributed in the cement paste. Therefore, the main task of constructing the meso-scale model of concrete is to determine the random aggregate structure (RAS) (Wang *et al*. 1999) according to some given parameters such as aggregate grading, volume content, etc. Currently, this topic has been widely discussed in many papers, especially in the field of the mechanic performance of concrete (Kim and Abu Al-Rub 2011). The shape of the aggregates has also been greatly developed, from two-dimensional circle (Bazant *et al*. 1990, Van Mier and Van Vliet 2003) to three-dimensional ellipsoid (Leite *et al*. 2004, Häfner *et al*. 2006) or polyhedron (Caballero *et al*. 2006) or even some other more complicated geometries with random boundary noise (Häfner *et al*. 2003). Although the three-dimensional RAS is already available, it is not often used in the analysis of the durability deterioration process of concrete, due to the difficulty in three-dimensional mesh and the tremendous calculation time and storage space of computers. According to some recently published papers (Zheng *et al*. 2012, Xu *et al*. 2012), a two-dimensional analysis is still popular and necessary. Furthermore, according to the stereology theory, the two-dimensional analysis can reflect the situation in three-dimensional space to some extent. Therefore, the research in this paper is conducted in two-dimension.

In two-dimension, the shape of the aggregates, especially the pebbles, can be simplified as an ellipse. The main reason for this simplification is that the elliptical particle is more flexible compared to a circular one and more convenient to control the shape compared with a polygonal one. Fig. 1 shows some real aggregates and their approximation results by elliptical particles.

$$\left(\frac{x'}{a}\right)^2 + \left(\frac{y'}{b}\right)^2 = 1 \tag{3}$$

where a and b are the major and minor radius of ellipse. The local coordinate of this ellipse can be transformed to the global coordinate by the following equation

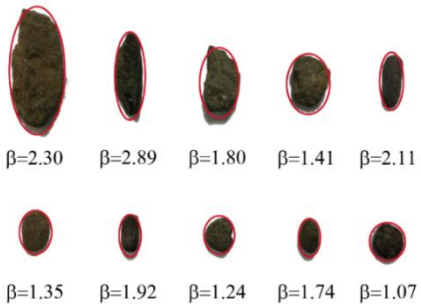

Fig. 1 Real aggregates and corresponding approximations by ellipse

$$(x, y, 1) = \left(x', y', 1\right) \cdot \begin{bmatrix} \cos(\alpha) & \sin(\alpha) & 0 \\ -\sin(\alpha) & \cos(\alpha) & 0 \\ 1 & 1 & 1 \end{bmatrix} \cdot \begin{bmatrix} 1 & 0 & 0 \\ 0 & 1 & 0 \\ x_0 & y_0 & 1 \end{bmatrix} \tag{4}$$

where α is the orientation of the ellipse, and (x_0, y_0) is the position of the ellipse's center in global coordinate.

To ensure that the generated elliptical particles can satisfy a given aggregate grading, a basic circular particle is first generated following the grading curve. This circular particle is then stretched into an ellipse. This approach is performed under the assumption that the area of the newly-formed ellipse is the same as that of the original circle (see Fig. 2). Hence, the major and minor radius of the elliptical particle can be calculated as follows

$$a = \sqrt{\beta} \cdot \frac{d}{2} \tag{5a}$$

$$b = \frac{d}{2} / \sqrt{\beta} \tag{5b}$$

where d is the diameter of the original circular particle, and $\beta = a/b$ is the aspect ratio of the elliptical particle.

2.2 Verification of the separation between the aggregates

As solid particles, aggregates are not allowed to overlap one another. Thus a separation check should be performed to determine the position of each aggregate. Wang *et al*. (2001) proved that two arbitrary ellipsoids are separated if and only if the following equation has two distinct positive roots.

$$f(\lambda) = 0 \qquad \text{with } f(\lambda) = \det(\lambda \mathrm{A} + \mathrm{B}) \tag{6}$$

where A and B are matrices describing the shape and position of ellipsoid by $\mathrm{X}^{\mathrm{T}}\mathrm{AX} = 0$, where $\mathrm{X} = (\mathrm{x}, \mathrm{y}, \mathrm{z}, 1)^{\mathrm{T}}$. Although this criterion was initially proposed for three-dimensional ellipsoids, it can also be used for two-dimensional ellipse by assuming that the third radius of ellipsoid to be infinite. The advantage of this separation criterion is its efficiency since only the signs of equation

roots are required.

As the aggregates are placed into the model, it becomes more difficult to find a proper position for the remaining aggregates. This difficulty is mainly due to the massive separation check for all existing aggregates. To improve the efficiency, the sub-domain method proposed by Häfner *et al*. (2006) is adopted in this paper. Within this method, the entire meso-scale model can be divided into several sub-domains. When the potential position of a new elliptical aggregate is randomly generated, the sub-domain where the aggregate lies or intersects is identified. Only the aggregates in the same sub-domain will be examined for the separation check. This method is especially efficient when a large area fraction of aggregates is needed.

2.3 Equivalent aggregate with interfacial transition zone

The interfacial transition zone (ITZ), a special region between the aggregate and cement paste, has a higher porosity than cement paste (Ollivier *et al*. 1995). Therefore, this region should not be ignored in a meso-scale model of concrete, especially for the purpose of chloride diffusion analysis. However, according to experimental observations (Ollivier *et al*. 1995, Scrivener and Nemati 1996), the thickness of ITZ (10~50μm) is much smaller than the diameter of an aggregate (which can be as large as 120mm). Such a significant difference in geometrical dimensions makes it difficult to generate a well-shaped mesh. Hence, it is not suitable to directly simulate the ITZ together with the aggregate. In this study, the theory proposed by Duan *et al*. (2006) is adopted, where the aggregate and the ITZ are modeled as an inclusion and a layer of uniform shell surrounding the inclusion, respectively.

The diffusivity of this composite material, i.e., equivalent aggregate can be obtained as follows

$$D_{x'} = D_{\mathrm{ITZ}} - \frac{(1+\beta)V_{\mathrm{agg}}}{V_{\mathrm{ITZ}} + (1+\beta)V_{\mathrm{agg}}} D_{\mathrm{ITZ}} \tag{7a}$$

$$D_{y'} = D_{\mathrm{ITZ}} - \frac{(1+\beta)V_{\mathrm{agg}}}{\beta V_{\mathrm{ITZ}} + (1+\beta)V_{\mathrm{agg}}} D_{\mathrm{ITZ}} \tag{7b}$$

where, V_{agg} and V_{ITZ} are the volume fractions of the aggregate and ITZ, respectively, and D_{ITZ} is the diffusivity of the ITZ. In the above equations, the chloride diffusion coefficient in the aggregate is equal to zero since porosity of the aggregate is much smaller than that of the ITZ and cement paste. The derived diffusion coefficient $D_{x'}$ and $D_{y'}$ are defined in the local coordinate as shown in Fig. 2. The diffusivity in global coordinate can be obtained by a tensor analysis (Zheng *et al*. 2012).

$$D_x = D_y = \frac{D_{x'} + D_{y'}}{2} \tag{8}$$

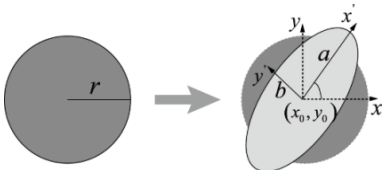

Fig. 2 Generation of elliptical aggregate from circle

3. Simulation method

3.1 Procedure of finite element analysis at meso-scale

The main purpose of the finite element analysis (FEA) at meso-scale is to determine the apparent chloride diffusion coefficient of concrete at macro-scale. The whole procedure of FEA can be conducted as follows:

(1) Generate the random elliptical aggregates in a two-dimensional meso-scale model.

(2) Mesh the geometry and generate input files for FEA.

(3) Determine the chloride diffusion coefficients in cement paste D_{cp} and ITZ D_{ITZ}.

(4) Apply the boundary conditions shown in Fig. 3 to the meso-scale model. The initial chloride concentration is assumed as zero.

(5) Perform a steady analysis to determine the distribution of chloride concentration in the model.

(6) Calculate the chloride flux in y-direction in each element J_i.

(7) The apparent diffusion coefficient of chloride can be determined based on the equivalent principle that the chloride flux in y-direction at meso-scale and at macro-scale should be the same to each other, i.e., $J_{\mathrm{me}} = J_{\mathrm{ma}}$, where $J_{\mathrm{me}} = \sum(J_i A_i)/\sum A_i$ and $J_{\mathrm{ma}} = D_{\mathrm{app}} \cdot C_{\mathrm{s}}/L$. A_i is the area of the element i. Hence,the apparent chloride diffusion coefficient in concrete can be calculated using thefollowing equation.

$$D_{\mathrm{app}} = \frac{\sum(J_i A_i)}{\sum A_i} \cdot \frac{L}{C_{\mathrm{s}}} \tag{9}$$

Since only steady state analysis is required in the above procedure, only the diffusion coefficient ratio $D_{\mathrm{ITZ}}/D_{\mathrm{cp}}$ instead of the absolute values of D_{ITZ} and D_{cp} is needed. Correspondingly, the final result is also given in the form of the diffusion coefficient ratio $D_{\mathrm{app}}/D_{\mathrm{cp}}$. Note that this parameter obtained by the above procedure is determined by FEA for a typical distribution of aggregates in the cement paste. If the distribution of aggregates changes, the result of $D_{\mathrm{app}}/D_{\mathrm{cp}}$ will also change, even if the other parameters such as the area fraction of aggregates are kept the same. This issue is quantitatively illustrated by a case study shown in Fig. 4. A series of 20 meso-scale models with different distributions of aggregates were generated, and the value of $D_{\mathrm{app}}/D_{\mathrm{cp}}$ for each model was calculated following the above procedure. As shown

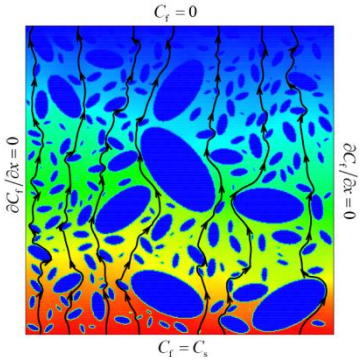

Fig. 3 Schematic illustration of boundary conditions at the meso-scale

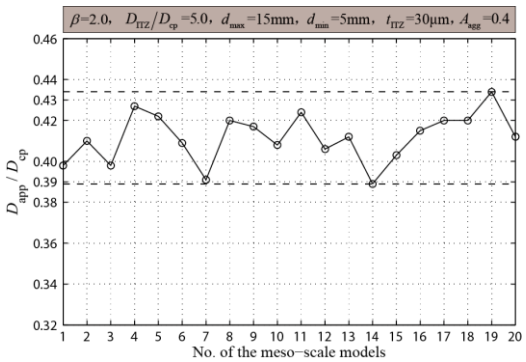

Fig. 4 Dependence of $D_{\text{app}}/D_{\text{cp}}$ on distribution of aggregates in cement paste

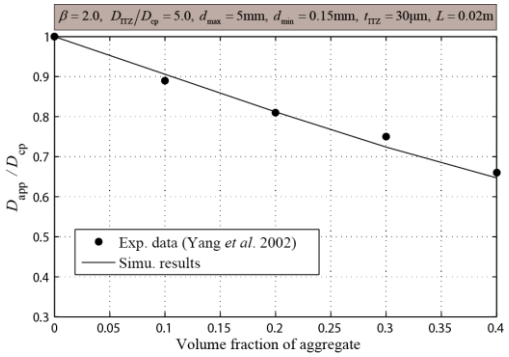

Fig. 5 Comparison with the experimental results

in Fig. 4, the value of $D_{\text{app}}/D_{\text{cp}}$ varied for different models. Since the other parameters remained constant, this variation was mainly due to the different distributions of aggregates in cement paste. In this case, the largest and smallest values of $D_{\text{app}}/D_{\text{cp}}$ obtained in the models were 0.434 and 0.389, respectively, with a relative difference of 11.57%, which should not be ignored.

Therefore, in order to obtain a more comprehensive understanding of the influence of aggregate on the chloride diffusivity in concrete, the above procedure should be repeated for different meso-scale models to obtain sufficient samples of $D_{\text{app}}/D_{\text{cp}}$. Based on statistical analysis of these samples, $D_{\text{app}}/D_{\text{cp}}$ can be considered as a random variable instead of a deterministic value.

3.2 Experimental verification

To verify the proposed numerical method, the experimental data by Yang and Su (2002) is adopted here. In their experiment, specimens with different aggregate area fractions, ranging from 0 to 0.4, were cast and the chloride diffusivity was determined by the migration test. The aggregate grading in this experiment is given in Fig. 7. Since the experiment report did not provide the information about the aggregate shape, the aspect ratio of the elliptical aggregates is supposed as $\beta = 2.0$ according to Zheng *et al*. (2012). As the thickness of ITZ was usually reported in the range of $10\sim50$ μm (Ollivier *et al*. 1995, Scrivener and Nemati 1996), t_{ITZ} is taken to be equal to 30 μm in this paper. The chloride diffusivity in ITZ cannot be directly measured in

experiments. However, it can be determined from the measured chloride diffusivities in two sets of specimens with different aggregate contents. According to the calculations in Zheng *et al*. (2012), $D_{\mathrm{ITZ}}/D_{\mathrm{cp}}$ can be considered to be equal to 5.0.

With the above parameters, the proposed numerical simulation method is used to evaluate the chloride diffusivity in the specimens in Yang and Su (2002). Considering the influence of random aggregate distribution on the simulation results, 100 meso-scale models are numerically generated for each specimen with a different aggregate content, and the final chloride diffusivity in concrete is obtained by averaging the results from these 100 meso-scale models. The comparison between simulation results and experiments results is shown in Fig. 5. From the comparison, it is verified that the numerical method proposed in this paper can reproduce the experimental results with reasonable accuracy.

4. Probability characteristics of $D_{\mathrm{app}}/D_{\mathrm{cp}}$

4.1 Random distribution

The previous discussion indicates that $D_{\mathrm{app}}/D_{\mathrm{cp}}$ should be considered as a random variable instead of a deterministic value. If the random distribution type of $D_{\mathrm{app}}/D_{\mathrm{cp}}$ can be found, the corrosion initiation time of the steel rebar can be predicted by the Monte Carlo method according to Eq. (1). Within the scope of this paper, the randomness of $D_{\mathrm{app}}/D_{\mathrm{cp}}$ mainly comes from the randomness of the meso-scale model of concrete, which can be influenced by many factors. First, the radius of the original circular aggregate r is randomly generated between r_{min} and r_{max} for a given aggregate grading. Second, orientation of elliptical aggregate is randomly generated to be uniform in the range of $0\sim2\pi$. Third, the position of the aggregate (x_0, y_0) is also randomly generated in cement paste. The interaction of these random variables makes it difficult to consider the randomness of the meso-scale model in an analytical approach. As a result, the random distribution type of $D_{\mathrm{app}}/D_{\mathrm{cp}}$ is difficult to identify. However, according to the central limit theorem (Billingsley 2012), the mean or sum of a sufficiently large number of independent random variables follows a normal distribution more or less. Hence, as a first approximation, a normal distribution might be an option.

Fig. 6 shows an example of fitting the samples of $D_{\mathrm{app}}/D_{\mathrm{cp}}$ using a normal distribution. In total, 100 samples of $D_{\mathrm{app}}/D_{\mathrm{cp}}$ were obtained by FEA for 100 meso-scale models. The normal probability plot, which gives a graphically illustration for whether the samples follow normal distribution, is shown in Fig. 6a. The straight dash line in the figure stands for an ideal normal distribution with an unknown mean μ and an unknown standard deviation σ. The closer the samples to this line, the more likely the samples will follow normal distribution. As indicated by the figure, $D_{\mathrm{app}}/D_{\mathrm{cp}}$ can be confidently regarded as a random variable following a normal distribution.

Hypothesis tests were also performed to evaluate the random distribution of $D_{\mathrm{app}}/D_{\mathrm{cp}}$. Two types of hypothesis tests were conducted to determine the normal distribution: the Jarque-Bera test (Jarque and Bera 1987) and Lilliefors test (Lilliefors 1967). The results of both tests indicate that $D_{\mathrm{app}}/D_{\mathrm{cp}}$ does not deny a normal distribution.

Based on the results of the graphical analysis above and the hypothesis tests, $D_{\mathrm{app}}/D_{\mathrm{cp}}$ can,

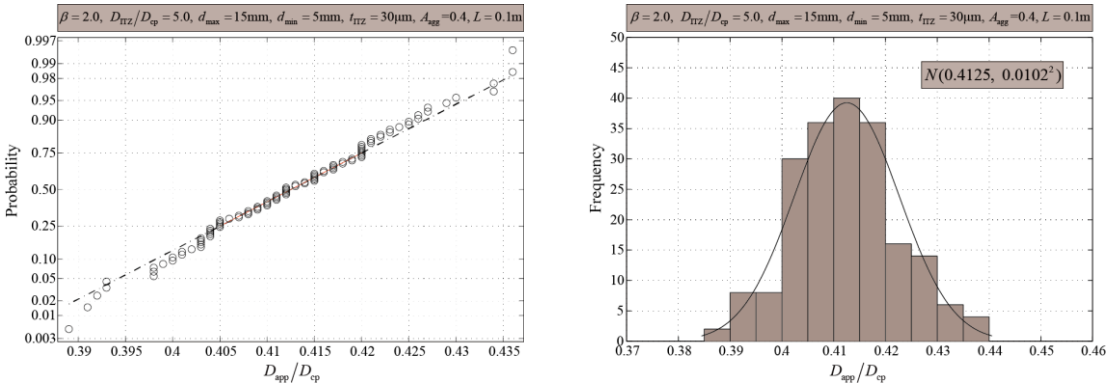

(a) Normplot (b) Normal distribution fitting

Fig. 6 Typical example on identification of random distribution of $D_{\text{app}}/D_{\text{cp}}$

with sufficient confidence, be considered as a random variable following a normal distribution, and the values of μ and σ of the normal distribution can be easily obtained by data fitting with the samples of $D_{\text{app}}/D_{\text{cp}}$ (as shown in Fig. 6b).

After the random distribution type of $D_{\text{app}}/D_{\text{cp}}$ is obtained, the random distribution type of D_{app} can be also determined. If $D_{\text{app}}/D_{\text{cp}}$ follows a normal distribution of $N(\mu,\sigma^2)$, D_{app} will follow $N\left(\mu\cdot D_{\text{cp}},\sigma^2\right)$, where D_{cp} is considered as a deterministic value.

4.2 Effect of aggregate grading

To study the effect of aggregate grading on $D_{\text{app}}/D_{\text{cp}}$, three different types of aggregate gradings shown in Fig. 7 are adopted. The main difference among these aggregate gradings is that type III grading has more small particles than type I, while type II lies between type III and type I.

The effect of these aggregate gradings on the probability characteristics of $D_{\text{app}}/D_{\text{cp}}$ is plotted in Fig. 8. Although the area fraction of aggregates is kept the same, different mean values of $D_{\text{app}}/D_{\text{cp}}$ are obtained for different aggregate gradings. This difference is mainly caused by

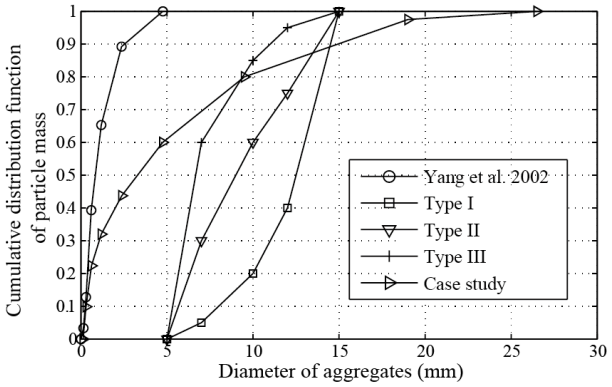

Fig. 7 Aggregate gradings used in this paper

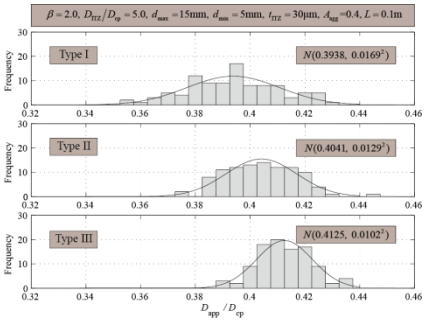

Fig. 8 Effect of aggregate grading on $D_{\text{app}}/D_{\text{cp}}$

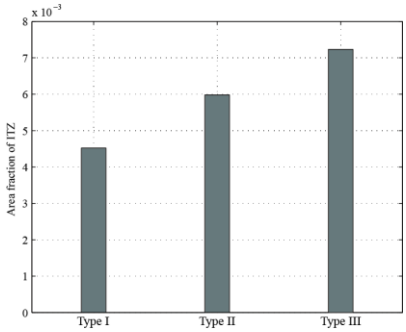

Fig. 9 Area fraction of ITZ in case study of Fig. 8

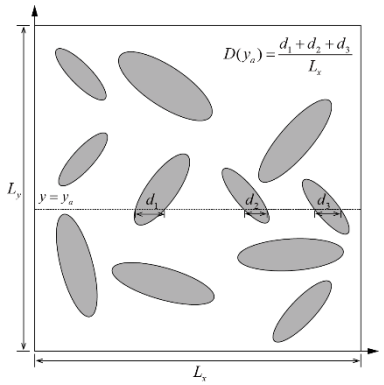

Fig. 10 Schematic illustration of $D(y)$

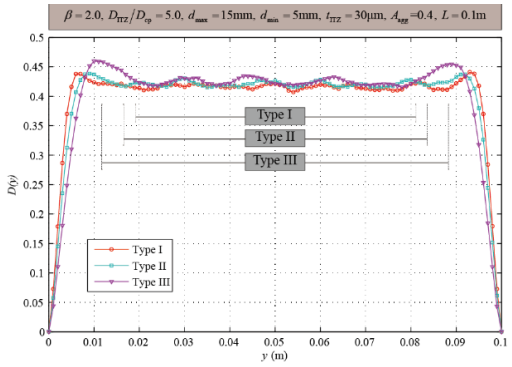

Fig. 11 $D(y)$ in case study of aggregate grading

the different area fractions of ITZ shown in Fig. 9. Due to a larger amount of small particles, the area fraction of ITZ with type III grading is larger, resulting in a larger μ of $D_{\text{app}}/D_{\text{cp}}$.

For the standard deviation of $D_{\text{app}}/D_{\text{cp}}$, it is also different for different aggregate gradings. As can be seem in Fig. 8, the standard deviation of the type III grading is smaller than that of type I. This tendency can be explained by the distribution density of aggregates $D(y)$. The definition of this parameter is schematically shown in Fig. 10, and detailed information about the calculation

method of this parameter can be found in Zheng *et al*. (2003). Generally, $D(y)$ is often used to present the local content of aggregates in two-dimension according to the theory of stereology.

The results of $D(y)$ in the above three cases are shown in Fig. 11. Due to the wall effect caused by the boundary of the meso-scale model, $D(y)$ near the boundary shows some degree of variation. However, in the inner part of the model, $D(y)$ reaches an almost stable value, resulting in a plateau of constant $D(y)$. As can be seem, the plateau of type III grading is wider than that of type I, indicating that the distribution of aggregates of type III grading is more homogeneous. Thus, the standard deviation of $D_{\text{app}}/D_{\text{cp}}$ of type III is smaller.

4.3 Effect of aggregate shape

In this study, the aggregates are simplified as elliptical particles. Therefore, the aspect ratio $\beta$is the only parameter that controls the shape of an aggregate. The influence of this parameter on $D_{\text{app}}/D_{\text{cp}}$ is plotted in Fig. 12, showing an obvious decreasing tendency of the mean value μ. This result agrees well with some earlier researches. For example, Granqvist and Hunderi (1978) used the extended Bruggemanns model to theorectically discusse the influence of the ellipsoid's shape on the conductivity of an effective-medium. Based on their findings, the effective-medium which has the ellipsoid particles with a larger β can have a lower conductivity. Another research is by Zheng *et al*. (2012) who used a lattice model to calculate the chloride diffusivity of concrete in a deterministic way. According to their numerical analysis, $D_{\text{app}}/D_{\text{cp}}$ decreases with an increase in β, which shows the same tendency as this paper. Both of these researches can support the result here.

Based on the above results, the aggregate with a larger β will result in higher resistance of concrete against the chloride ions. Therefore, this kind of aggregate has the potential to be preferred in practice, at least from the perspective of durability performance of concrete. However, this conclusion is only obtained through an investigation of the mean value μ. For the standard deviation σ, it increases with β, an opposite tendency with μ, as shown in Fig. 12. This difference indicates that if one uses a deterministic approach to predict the chloride diffusion process, i.e., using only μ to calculate the chloride concentration without considering σ, there is an increased possibility that the prediction of chloride concentration will fail for the aggregate with a larger β (see Fig. 13 for a clearer understanding of this issue). Therefore, from the probabilistic point of view, theaggregate with a large β should be avoided.

Another disadvantage of using the aggregate with a larger β is that such aggregate will contribute to more severe anisotropy of concrete. In ideal conditions, the chloride diffusivity in the *x*-direction D_x and *y*-direction D_y should be exactly the same for an isotropic material. This is widely adopted in current macroscopic research on chloride diffusion process. However, in meso-scale analysis, the non-uniformly distribution of aggregates in cement paste will make the concrete anisotropic, resulting in different values of D_x and D_y. Similar to $D_{\text{app}}/D_{\text{cp}}$, D_x/D_y can also be considered as a random variable. This issue is illustrated by the case study shown in Fig. 14. For aggregates with three different values of β, the mean values of D_x/D_y are almost the same and approximately equal to 1.0, which is the case for isotropic materials. In the other aspect, the standard deviations of D_x/D_y are different from one another with an increasing tendency with β, indicating a higher possibility of anisotropic properties of the concrete (see Fig. 13).

The above discussion on the anisotropic property of concrete at meso-scalecan be further

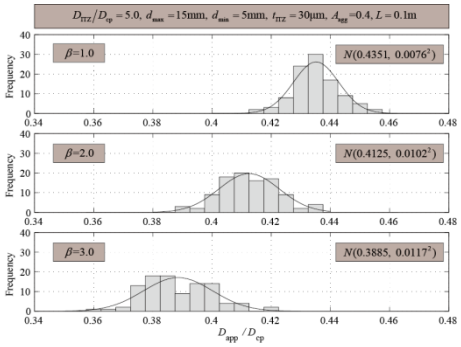

Fig. 12 Effect of aggregate shape on $D_{\mathrm{app}}/D_{\mathrm{cp}}$

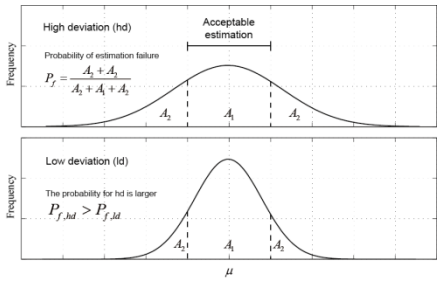

Fig. 13 Relationship between deviation of random variable and corresponding probability of estimation failure

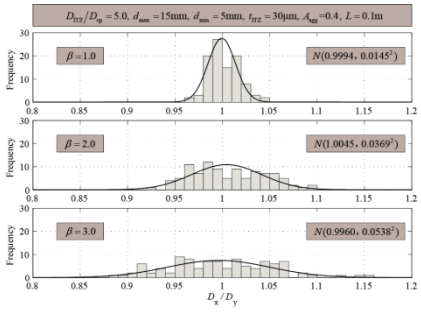

Fig. 14 Influence of aggregate shape on anisotropy of concrete

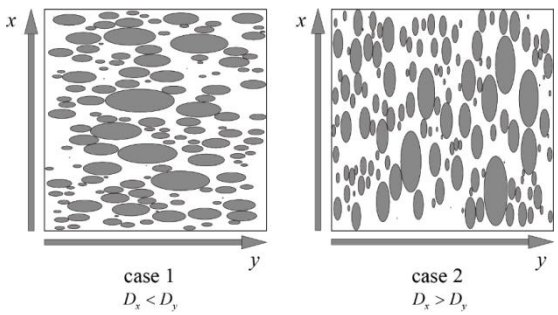

Fig. 15 A schematic of extreme distributions of aggregates in meso-scale model

explained. In a very extreme condition, all the aggregates can be distributed in the cement paste with a uniform orientation of zero (case 1 in Fig. 15) or $\pi/2$ (case 2 in Fig. 15). In case 1, it is obvious that the chloride diffusivity in the *x*-direction D_x and *y*-direction D_y has the relationship of $D_x < D_y$, since the meso-scale model of case 1 has a higher ability to impede the chloride ions in the *x*-direction. When the orientation of aggregates increases, D_x will decrease while D_y will increase, which can eventually decrease the ratio of D_x/D_y. In case 2, the result is just opposite. In reality, the true distribution of aggregates will absolutely drop between case 1 and case 2. As a result, when the orientation β increases, a larger standard deviation of D_x/D_y will be expected. Therefore, a more anistropic concrete will be produced in a probabilistic sense.

Based on the above discussions, from the probabilistic point of view there are two opposite aspects in the influence of aggregate shape on $D_{\text{app}}/D_{\text{cp}}$, which makes it difficult to decide which should be used in practice. According to the statistical analysis of real aggregates, Wang *et al*. (2005) found that β of common aggregates was around 2.0. Therefore, the aggregate with $\beta > 2.0$ may not be recommended. In addition, the aggregate with a larger β may be more likely to cause a severe stress concentration in concrete. As a result, from the perspective of mechanical performance, the aggregate with a large β should also be avoided.

4.4 Size effect at meso-scale

Size effect is a common phenomenon of concrete. The same experiment on concrete specimens with different sizes can produce different results. This phenomenon does not only exists in the mechanical properties such as elastic module and compressive strength which has been widely discussed in many papers (Bazant and Planas 1997), but also exists in the properties related with the durability performance like chloride diffusivity, especially from a probabilistic point of view.

Fig. 16 shows the results of a case study on the size effect. The lengths of meso-scale models are set to be 0.05 m, 0.10 m, and 0.15 m, respectively. Based on the results, the mean values of $D_{\text{app}}/D_{\text{cp}}$ for different meso-scale models are almost the same. However, the standard deviation decreases when the size of the meso-scale model increases.

The above tendency can be also explained by the distribution density of aggregates $D(y)$. Fig. 17 shows the results of $D(y)$ in the three cases in Fig. 16. In the cases of $L = 0.10\text{m}$ and $L = 0.15\text{m}$, a plateau with a almost constant $D(y)$ can be found, and the width of this plateau increased with the size of the meso-scale model. For the case of $L = 0.05\text{m}$, no such plateau was found. These results indicate that in the models with larger size, the distribution of aggregates in cement paste will be more homogeneous, resulting in a smaller standard deviation of $D_{\text{app}}/D_{\text{cp}}$. Therefore, for large-scale infrastructures such as concrete dam, the probabilistic issue of $D_{\text{app}}/D_{\text{cp}}$ can be ignored, and a deterministic approach can be used to calculation the chloride concentration with the mean value μ.

However, the situation is different for RC structures since the rebar in the concrete can significantly influence the distribution of aggregates in cement paste. To quantitatively evaluate this effect, a case study was conducted in which a 16mm-diameter rebar was embedded in concrete with a 40mm-thick protective layer. $D(y)$ in this case is shown in Fig. 18. Although a similar plateau of $D(y)$ can be found in the region behind the rebar, $D(y)$ in the protective layer shows a lot of variation. This kind of variation can increase the uncertainty of the chloride diffusion process in the protective layer, while the plateau of $D(y)$ found behind the rebar is of no

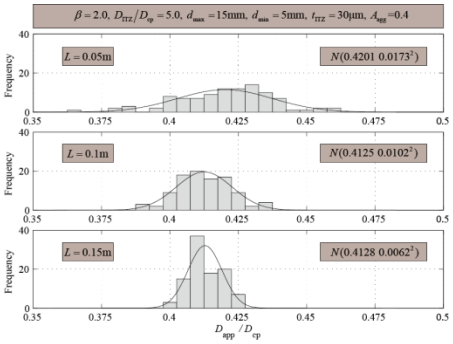

Fig. 16 Size effect of meso-scale model on $D_{\text{app}}/D_{\text{cp}}$

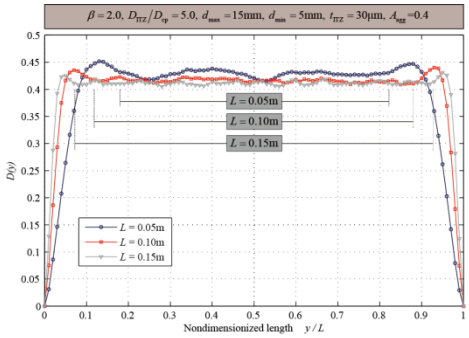

Fig. 17 $D(y)$ in case study of Fig. 16

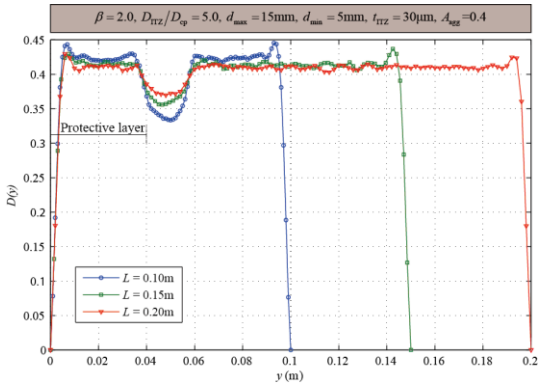

Fig. 18 Influence of steel rebar on $D(y)$

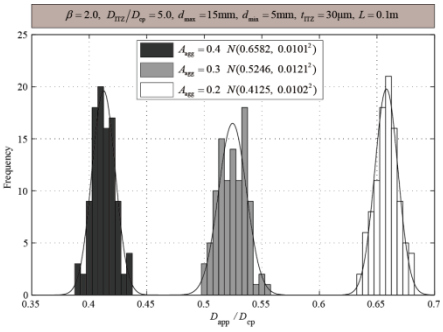

Fig. 19 Effect of aggregate content on $D_{\text{app}}/D_{\text{cp}}$.

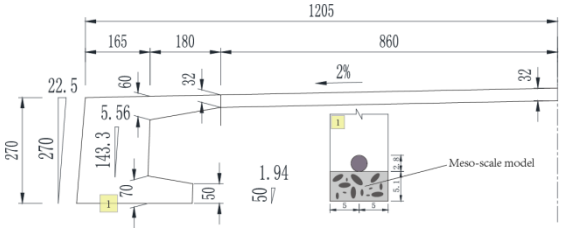

Fig. 20 Cross section of main girder (cm)

significance. Therefore, to predict the chloride diffusion process in RC members, the size of the model where meso-scale analysis is performed should not be very large. Otherwise, the standard deviation of $D_{\mathrm{app}}/D_{\mathrm{cp}}$ may be underestimated.

According to the above discussion, it is important to determine a proper model size for the simulation to make the standard deviation of $D_{\mathrm{app}}/D_{\mathrm{cp}}$ a meaningful and explicit parameter for practical application.Based on the analysis of Fig. 16, it can be concluded that the the size effect is mainly caused by the unstable area ratio of aggregates near the boundary of the meso-scale model. When the boundary has a larger influencing area, such as the case of $L = 0.05\mathrm{m}$ in Fig. 16, a larger standard deviation of $D_{\mathrm{app}}/D_{\mathrm{cp}}$ will be obtained. In RC structures, the boundary near the surface of steel rebars can also influence the distribution density of aggregates and a dropping of $D(y)$ can be found in this region, as shown in Fig. 17. In this sense, the boundary of steel rebars has a similar effect with the boundary of the meso-scale model, although the former effect is not as obvious as the latter one. Therefore, the depth of the protective layer should be chosen as the proper size of the meso-scale model. This approach is also reasonable in that the chloride diffusion process in the protective layer is usually the main concern in practical engineering.

4.5 Effect of aggregate content

The effect of aggregate content (expressed as area ratio A_{agg} in two-dimension) on $D_{\mathrm{app}}/D_{\mathrm{cp}}$ is plotted in Fig. 19. As can be seen, the mean value of $D_{\mathrm{app}}/D_{\mathrm{cp}}$ decreases with an increase in A_{agg}, indicating that the concrete with a higher content of aggregates has a better resistance to chloride ions. This result agrees with current empirical models and is reasonable, because the tortuosity effect of aggregates on the chloride diffusion process is more significant for the cases with a larger area ratio of aggregates. Meanwhile, the standard deviation σ does not show obvious variation along with the area ratio of aggregates. Therefore, from the perspective of μ, the aggregate should be sufficiently used to decrease the permeability of concrete. However, of course, the proper content of aggregate should be decided with other considerations, e.g., workability of concrete.

5. Practical application

The initiation time of steel corrosion is a very important index to represent the durability performance of RC structures. Sometimes, it can be referred as the life time of important RC members, where the steel rebars are not permitted to corrode. According to Eq. (1), since the apparent chloride diffusion coefficient D_{app} is viewed as a random variable, the corrosion initiation time T_{corr} should be also considered as a random variable, and the probabilistic characteristics of T_{corr}, e.g., distribution type, mean value, standard deviation, can be easily obtained according to that of D_{app} by the Monte Carlo simulation method.

To illustrate the application of the mesoscopic method developed in this paper in the prediction of corrosion initiation time of RC members, the chloride diffusion process in the main girder of a cable-stayed bridge is analyzed. Half of the π shaped cross section of this girder is shown in Fig. 19. Since the chloride diffusion process is very slow and usually happens near the surface of RC members, only a small region cut from the entire cross section is analyzed in order to enhance the

Table 1 Mix proportion of concrete

	Cement	Water	Fine aggregate*	Coarse aggregate*
Quality ratio	1.00	0.36	2.48	1.27
Density ($\times 10^3$ kg/m^3)	3.15	1.00	2.70	2.70
Volume ratio	1.00	1.13	2.89	1.48

*The grading of aggregate is shown in Fig. 7.

Table 2 Calculation of D_{cp}

Variable	Influence function	Result	Reference
T	$f_{\mathrm{T}}(T) = exp\left[\frac{U}{R}\left(\frac{1}{273}-\frac{1}{T}\right)\right]$	1.00	Xi and Bazant (1999)
h	$f_{\mathrm{h}}(h) = \left[1+\frac{(1-h)^4}{(1-0.75)^4}\right]^{-1}$	0.71	Ababneh *et al*. (2003)
C_{f}	$f_{\mathrm{b}}(C_{\mathrm{f}}) = (dC_{\mathrm{t}}/dC_{\mathrm{f}})^{-1}$	0.86[a]	Mohammed and Hamada (2003)
σ	-	1.10[b]	CECS 220 (2007)

[a]Although nonlinear chloride binding isotherm is often reported in laboratory experiments, the relationship between free chloride and total chloride concentrations in field-exposed concrete is linear. See Yuan *et al*. (2009) for more information.

[b]Currently, it is difficult to discuss the influence of stress on the chloride diffusion coefficient quantitatively. Therefore, only a qualitative approach is adopted here.

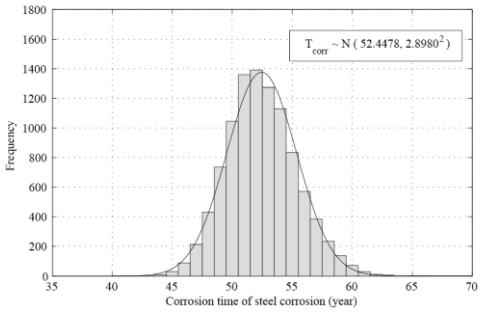

Fig. 21 Probabilistic distribution of corrosion initiation time of initial design scheme

calculation efficiency. The size of the region, as well as the diameter of steel rebar, the depth of protective layer is also shown in Fig. 19. The mix proportion and the aggregate grading of the concrete used in this girder are shown in Table 1 and Fig. 7 (the grading curve labelled as "case study"), respectively.

As pointed out in the beginning of this paper, a lot of factors can influence the chloride diffusion coefficient. In this example, only the factors of water cement ratio, curing time, temperature, relative humidity, chloride binding, stressed condition and of course aggregate are considered. The influences of all the factors except aggregate on the chloride diffusion coefficient

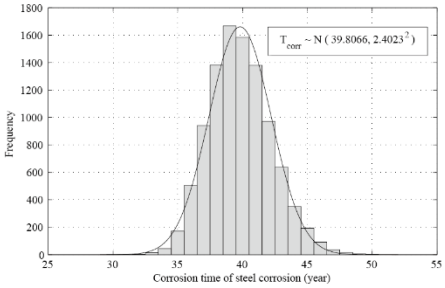

(a) $d = 4.5$cm

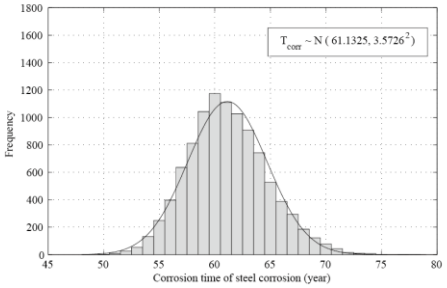

(b) $d = 5.5$cm

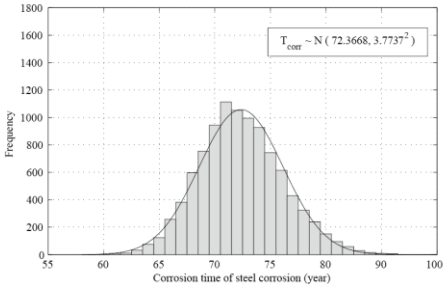

(c) $d = 6.0$ cm

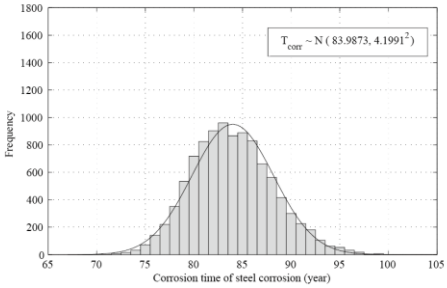

(d) $d = 6.5$ cm

Fig. 22 Probabilistic distribution of corrosion initiation time of other design schemes withdifferent protective layers

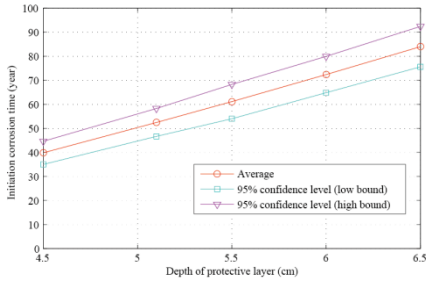

Fig. 23 Average and 95% confidence level of corrosion initiation time of different protective layers

are assessed in a deterministic way. Following this idea, Eq. (2) should be rewritten as

$$D_{\text{app}} = D_{\text{cp}}(\text{w/c}, t_0, T, h, C_{\text{f}}, \sigma) \cdot f_a \tag{10}$$

where

$$D_{\text{cp}} = D_{\text{cp},0}(\text{w/c}, t_0) \cdot f_{\text{T}}(T) \cdot f_{\text{h}}(h) \cdot f_{\text{b}}(C_{\text{f}}) \cdot f_{\sigma}(\sigma) \tag{11}$$

The model proposed by Xi and Bazant (1999) is used to calculate $D_{\text{cp},0}$. This model, as shown in Eq. (12) has already considered the effects of water cement ratio and curing time on the chloride diffusion coefficient. The influences of the other factors are assessed in Table 2.

$$D_{\mathrm{cp},0} = \frac{28-t_0}{62500} + \left[\frac{1}{4} + \frac{28-t_0}{300}\right](\mathrm{w/c})^{6.55} = 3.14 \times 10^{-4}\ \mathrm{m^2/a} \quad (12)$$

The effect of aggregates on the chloride diffusion coefficient is evaluated by the mesoscopic method in this paper. Totally 500 meso-scale models are numerically generated. The size of the mesoscopic model is the same with the depth of the protective layer (see Fig. 20). Following the FEA procedure introduced in Section 3.1, 500 corresponding samples of $D_{\mathrm{app}}/D_{\mathrm{cp}}$ are obtained. By fitting the results with normal distribution, the mean value and standard deviation of $D_{\mathrm{app}}/D_{\mathrm{cp}}$ can be determined. After that, the initiation time of steel corrosion can be calculated using Eq. (1) by the Monte Carlo method. During this calculation, the surface and threshold chloride concentrations should be known. According to CECS220 (2007), the surface chloride concentration is $C_{\mathrm{s}}^{\mathrm{f}} = 1.4\,\mathrm{kg/m^3}$, based on the location of this bridge, while the threshold chloride concentration is $C_{\mathrm{s}}^{\mathrm{f}} = 3.2\,\mathrm{kg/m^3}$, which is related with the material itself.

The final result of the corrosion initiation time is shown in Fig. 21. As can be seen, the steel rebar is likely to start corroding in the 52nd year in the average sense. Following the same procedure above, the corrosion initiation time of different depths of the protective layer can be also obtained, as shown in Fig. 22. The average corrosion initiation time and the 95% confidence levels of all these protective layers are summarized in Fig. 23. It can be seen that both of the average and standard deviation of the corrosion initiation time will increase with the depth of the protective layer. This tendency indicates that although a thicker protective layer can effectively delay the corrosion of steel rebars, it can also make the prediction less reliable at the same time. Therefore, it is better to adopt a probabilistic approach to predict the corrosion initiation time of steel rebarsespecially for the RC structures with a longer expected life and a thicker protective layer. Furthermore, it should be pointed out that the uncertainty of the predicted corrosion initiation time may be accumulated and increased if the probabilistic characteristics of the temperature, relative humidity, etc. are also considered when the environmental conditions change intensively. In this case, a probabilistic approach is of special necessity.

6. Conclusions

This paper applies a probabilistic analysis to study the chloride diffusion process at meso-scale by the chloride diffusion coefficient ratio $D_{\mathrm{app}}/D_{\mathrm{cp}}$. The simulation method of random elliptical aggregates and the procedure of mesoscopic FEA are introduced. Furthermore, the random distribution of $D_{\mathrm{app}}/D_{\mathrm{cp}}$ is determined, and the effect of aggregates, including aggregate grading, shape, size of meso-scale model, and aggregate content is discussed. Based on the results and discussions, the following conclusions can be drawn.

(1) $D_{\mathrm{app}}/D_{\mathrm{cp}}$ can be viewed, with confidence, as a random variable following a normal distribution.

(2) The aggregate grading which contains more small particles can result in a larger average of $D_{\mathrm{app}}/D_{\mathrm{cp}}$ due to the larger area fraction of ITZ. Meanwhile, the standard deviation of $D_{\mathrm{app}}/D_{\mathrm{cp}}$ may decrease along with the content of the small particles in the aggregate grading.

(3) Aggregates with a larger aspect ratio β can decrease the permeability of concrete on average. However, the standard deviation of $D_{\mathrm{app}}/D_{\mathrm{cp}}$ will increase with, indicating a higher probability of estimation failure. In addition, the concrete is more likely to be anisotropic when the aggregates with a larger β are used.

(4) The size of the model used in the mesoscopic analysis has a close relationship with the standard deviation of $D_{\text{app}}/D_{\text{cp}}$. Generally, the larger the model is, the smaller the standard deviation of $D_{\text{app}}/D_{\text{cp}}$ will be. In RC members, the property size of the meso-scale model is recommended to be equal to the size of the protect-layer of steel rebars.

(5) A higher content of aggregates can greatly decrease the chloride diffusivity in mortar or concrete, while the standard deviation of $D_{\text{app}}/D_{\text{cp}}$ shows no significant change.

Besides the above conclusions, this paper provides a deeper insight into the mesoscopic study of the durability performance of concrete, and forwards the current deterministic research into a probabilistic one in this field.

Acknowledgements

The research is partially supported by the Fundamental Research Funds for the Central Universities (Tongji University) of China, the National Science Foundation of China (Grant No. 51378383), the Guizhou traffic science and technology project of China (Grant No. 2010-122-018), and the Jiangxi traffic science of technology project of China (Grant No. 2010C00012). The first author appreciates the China Scholar Council (CSC) for supporting his visiting research experience in University of California at Berkeley and Prof. Monteiro P.J.M. for suggestions on this paper.

References

Ababneh, A., Benboudjema, F. and Xi, Y. (2003), "Chloride penetration in nonsaturated concrete", *J. Mater. Civil Eng.*, **15**(2), 183-191.

Almusallam, A.A., Al-Gahtani, A.S., Aziz, A.R., Rasheeduzzafar (1996), "Effect of reinforcement corrosion on bond strength", *Constr. Build.Mater.*, **10**(2), 123-129.

Bazant, Z.P. and Planas, J. (1997), *Fracture and Size Effect in Concrete and Other Quasi-brittle Materials*, CRC PressILlc.

Bazant, Z.P., Tabbara, M., Kazemi, M., and Pijaudier-Cabot, G. (1990), "Random particle model for fracture of aggregate or fiber composites", *J. Eng. Mech.*, **116**(8), 1686-1705.

Bentz, D.P. (2007), "A virtual rapid chloride permeability test", *Cement Concrete Compos.*, **29**(10), 723-731.

Billingsley, P. (2012), "*Probability and measure*", John Wiley & Sons.

Caballero, A., López, C. and Carol, I. (2006), "3D meso-structural analysis of concrete specimens under uniaxial tension", *Comput. Meth. Appl. Mech. Eng.*, **195**(52), 7182-7195.

Cabrera, J. (1996), "Deterioration of concrete due to reinforcement steel corrosion", *Cement Concrete Compos.*, **18**(1), 47-59.

Cairns, J., Plizzari, G.A., Du, Y., Law, D.Y. and Franzoni, C. (2005), "Mechanical properties of corrosion-damaged reinforcement", *ACI Mater. J.*, **102**(4), 256-264.

Caré, S. and Hervé, E. (2004), "Application of a n-phase model to the diffusion coefficient of chloride in mortar", *Transport in porous media*, **56**(2), 119-135.

Caré, S. (2003), "Influence of aggregates on chloride diffusion coefficient into mortar", *Cement Concr. Research*, **33**(7), 1021-1028.

CECS220 (2007), Standard for durability assessment of concrete structures (CECS220:2007), China Construction Press.

Chen, D. and Mahadevan, S. (2008), "Chloride-induced reinforcement corrosion and concrete cracking

simulation", *Cement Concrete Compos*., **30**(3), 227-238.
Du, Y., Clark, L. and Chan, A. (2005), "Residual capacity of corroded reinforcing bars", *Mag*. *Concrete Res*., **57**(3), 135-148.
Duan, H.*et al*. (2006), "Effective conductivities of heterogeneous media containing multiple inclusions with various spatial distributions", *Phys*. *Review B*, **73**(17), 174203.
Garboczi, E. and Bentz, D. (1992), "Computer simulation of the diffusivity of cement-based materials", *J*. *Mater*. *Sci*., **27**(8), 2083-2092.
Granqvist, C. and Hunderi, O. (1978), "Conductivity of inhomogeneous materials: effective-medium theory with dipole-dipole interaction", *Phys*. *Review B*, **18**(4), 1554.
Häfner, S., Eckardt, S. and Könke, C. (2003), "A geometrical inclusion-matrix model for the finite element analysis of concrete at multiple scales. In: Proceedings of the 16th IKM.
Häfner, S., *Eckardt*, *S*., *Luther*, *T*., *Könke*, *C*. (2006), "Mesoscale modeling of concrete: geometry and numeric", *Comput*. *Struct*., **84**(7), 450-461.
Halamickova, P. Detwiler, R.J., Bentz, D.P. and Garboczi, E.J. (1995), "Water permeability and chloride ion diffusion in Portland cement mortars: relationship to sand content and critical pore diameter", *Cement Concrete Res*., **25**(4), 790-802.
Han, S.H. (2007), "Influence of diffusion coefficient on chloride ion penetration of concrete structure", *Constr*.*Build*. *Mater*., **21**(2), 370-378.
Hobbs, D. (1999), "Aggregate influence on chloride ion diffusion into concrete", *Cement Concrete Res*., **29**(12), 1995-1998.
Jarque, C. and Bera, A. (1987),"A test for normality of observations and regression residuals", International Statistical Review/Revue Internationale de Statistique, 163-172.
Kim, S.M. and Abu Al-Rub, R.K. (2011),"Meso-scale computational modeling of the plastic-damage response of cementitious composites", *Cement Concrete Res*., **41**(3), 339-358.
Leite, J., Slowik, V. and Mihashi, H. (2004),"Computer simulation of fracture processes of concrete using mesolevel models of lattice structures", *Cement Concrete Res*., **34**(6), 1025-1033.
Li, L.Y., Xia, J. and Lin, S.S. (2012),"A multi-phase model for predicting the effective diffusion coefficient of chlorides in concrete", *Constr*. *Build*. *Mater*., **26**(1), 295-301.
Lilliefors, H. (1967), "On the Kolmogorov-Smirnov test for normality with mean and variance unknown", *J*. *the American Statistical Assoc*.,**62**(318), 399-402.
Mohammed, T. and Hamada, H. (2003),"Relationship between free chloride and total chloride contents in concrete",*Cement Concr*. *Res*.**33**(9), 1487-1490.
Oh, B.H. and Jang, S.Y. (2004),"Prediction of diffusivity of concrete based on simple analytic equations", *Cement Concrete Res*., **34**(3), 463-480.
Ollivier, J., Maso, J. and Bourdette, B. (1995),"Interfacial transition zone in concrete", *Advanced Cement Based Mater*., **2**(1), 30-38.
Ruan, X. and Pan, Z.C. (2012), "Mesoscopic simulation method of concrete carbonation process", *Struct*. *Infrastruct*. *Eng*., **8**(2), 99-110.
Saetta, A.V. (2005), "Deterioration of reinforced concrete structures due to chemical–physical phenomena: model-based simulation", *J*. *Mater*. *Civil Eng*., **17**(3), 313-319.
Scrivener, K.L. and Nemati, K.M. (1996), "The percolation of pore space in the cement paste/aggregate interfacial zone of concrete", *Cement Concrete Res*., **26**(1), 35-40.
Shafei, B., Alipour, A. and Shinozuka, M. (2011), "Prediction of corrosion initiation in reinforced concrete members subjected to environmental stressors: A finite-element framework", *Cement Concrete Res*., **42**(2), 365-376.
Van Mien, T., Stitmannaithum, B. and Nawa, T. (2011), "Prediction of chloride diffusion coefficient of concrete under flexural cyclic load", *Comput*. *Concr*., **8**(3), 343-355.
Van Mier, J. and Van Vliet, M. (2003), "Influence of microstructure of concrete on size/scale effects in tensile fracture", *Eng*. *Fracture Mech*., **70**(16), 2281-2306.
Wang, L. and Ueda, T. (2011), "Mesoscale simulation of chloride diffusion in concrete considering the

binding capacity and concentration dependence", *Computers Concr*., **8**(3), 125-142.
Wang, L., Wang, X., Mohammad, L. and Abadie, C. (2005), "Unified method to quantify aggregate shape angularity and texture using fourier analysis", *J. Mater. In civil Eng*., **17**(5), 498-504.
Wang, W., Wang, J. and Kim, M. (2001), "An algebraic condition for the separation of two ellipsoids", *Computer aided geometric design*, **18**(6), 531-539.
Wang, X.Y., Park, K.B. and Lee, H.S. (2012), "Modeling of chloride diffusion in a hydrating concrete incorporating silica fume", *Comput. Concr*., **10**(5), 523-539.
Wang, Z., Kwan, A. and Chan, H. (1999), "Mesoscopic study of concrete I: generation of random aggregate structure and finite element mesh", *Comput. Struct*., **70**(5), 533-544.
Xi, Y. and Bazant, Z.P. (1999), "Modeling chloride penetration in saturated concrete", *J. Mater. Civil Eng*., **11**(1), 58-65.
Xu, Z., Hao, H. and Li, H. (2012), "Mesoscale modelling of fiber reinforced concrete material under compressive impact loading", *Constr. Build. Mater*., **26**(1), 274-288.
Yang, C. (2005), "Effect of the percolated interfacial transition zone on the chloride migration coefficient of cement-based materials", *Mater. Chem. Phys*., **91**(2), 538-544.
Yang, C. and Su, J. (2002), "Approximate migration coefficient of interfacial transition zone and the effect of aggregate content on the migration coefficient of mortar", *Cement Concrete Res*., **32**(10), 1559-1565.
Yuan, Q., Shi, C., Schutterc, G.D., Audenaertc, K. and Denga, D. (2009), "Chloride binding of cement-based materials subjected to external chloride environment–a review", *Construct. Build. Mater*., **23**(1), 1-13.
Zeng, Y. (2007), "Modeling of chloride diffusion in hetero-structured concretes by finite element method", *Cement Concrete Compos*., **29**(7), 559-565.
Zhang, S.P. and Zhao, B.H. (2012), "Research on chloride ion diffusivity of concrete subjected to CO_2 environment", *Comput. Concr*., **10**(3), 219-229.
Zhang, S.P., Dong, X and Jiang, J.Y. (2013), "Effect of measurement method and cracking on chloride transport in concrete", *Comput. Concr*., **11**(4), 305-316.
Zheng, J.J., Zhou, X.Z., Wu, Y.F. and Jin, X.Y. (2012), "A numerical method for the chloride diffusivity in concrete with aggregate shape effect", *Constr. Build. Mater*., **31**, 151-156.
Zheng, J. and Zhou, X. (2008), "Three-phase composite sphere model for the prediction of chloride diffusivity of concrete", *J. Mater. Civil Eng*., **20**(3), 205-211.
Zheng, J., Li, C. and Zhao, L. (2003), "Simulation of two-dimensional aggregate distribution with wall effect", *J. Mater. Civil Eng*., **15**(5), 506-510.

CC